

# Singular evanescent wave resonances

Yu Guo and Zubin Jacob\*

Department of Electrical and Computer Engineering,  
University of Alberta, Edmonton, Alberta, T6G 2V4, Canada

\*[zjacob@ualberta.ca](mailto:zjacob@ualberta.ca)

## Abstract

Resonators fold the path of light by reflections leading to a phase balance and thus constructive addition of propagating waves. However, amplitude decrease of these waves due to incomplete reflection or material absorption leads to a finite quality factor of all resonances. Here we report on our discovery that evanescent waves can lead to both a phase and amplitude balance causing an ideal Fabry-Perot resonance condition in spite of material absorption and non-ideal boundary discontinuities. We show that this singular resonance can be spontaneously excited between moving bodies separated by a small gap causing infinitely many photons to be exchanged between them. Furthermore, we also show that the momentum transfer due to these photons can lead to a divergent vacuum friction between the moving bodies.

## Introduction

The canonical example of a resonator is the Fabry-Perot (FP) system consisting of two reflecting plates separated by a vacuum gap [1,2]. Light bouncing between them not only serves as a textbook introduction to the concept of a resonance but is the basis of practical devices from the laser to the interferometer [1,2]. A simple argument often suffices to understand this resonance. The reflection coefficient of propagating waves with frequency  $\omega$  from the first mirror ( $r_1(\omega)$ ) times that of the second mirror ( $r_2(\omega)$ ) along with the propagation phase accumulated over a round trip ( $e^{2ik_z d}$ ) should reconstruct the wave, capturing it inside, leading to a resonant build-up of intensity. Here,  $d$  is the vacuum gap between the two mirrors and  $k_z$  is the propagation constant perpendicular to the mirrors. We arrive at the well-known Fabry-Perot resonance condition

$$r_1(\omega)r_2(\omega)e^{2ik_z d} = 1, \quad (1)$$

which also follows from a plane wave multiple scattering approach. Note that the reflection coefficients are complex signifying the change in phase and amplitude of the propagating wave at the mirrors. A closer look reveals that an optimum choice of the gap can possibly lead to a net phase balance ( $\arg(r_1(\omega)r_2(\omega)e^{2ik_z d}) = 2n\pi$ ) for a resonance, but material absorption and non-ideal reflections necessarily require  $|r_1(\omega)r_2(\omega)| < 1$  (Fig. 1a). A gain medium is needed to compensate for this loss in amplitude as in a laser. The arguments presented above can be generalized to arbitrary passive structures showing that the bound resonances are signified by the poles of the scattering matrix which always lie in the lower half ( $\text{Im}(\omega_{res}) < 0$ ) of the complex frequency plane [3]. This condition ensures that all resonances decay in time leading to a finite quality factor.

## Perfect phase and amplitude balance

The case for evanescent waves in such a configuration is interestingly different. They do not have phase propagation and the amplitude of such waves exponentially decays within the vacuum gap. Furthermore, those evanescent waves which couple to the surface modes of the mirror can have a reflection coefficient with amplitude greater than unity (Fig. 1b). Such waves can thus have  $|r_1(\omega)r_2(\omega)| > 1$  to compensate the evanescent decay within the gap as well as non-

ideal mirror reflections. The important condition of phase balance however still remains since the mirrors necessarily impart a phase change to the evanescent waves which cannot be compensated while propagating. We also note that the mirrors cannot balance or cancel the phase imparted to the evanescent wave by each other irrespective of their dielectric properties. This can be discerned by studying the energy of incident evanescent waves on any medium given by the normal component of the Poynting vector (see Supplementary Information)

$$S_z = \frac{1}{2} \text{Re}(E \times H^*)_z = \frac{|k_z|}{2\omega\mu_0} 2 \text{Im}(r). \quad (2)$$

For passive media, the energy tunneling into the medium is positive ( $S_z > 0$ ,  $\text{Im}(r) > 0$ ) implying that the complex reflection coefficient of evanescent waves lies in the upper half of the complex plane and  $0 < \arg(r(\omega)) < \pi$ . Thus the product of the reflection coefficients at the two mirrors cannot be purely real for evanescent waves as required for resonance ( $0 < \arg(r_1(\omega)r_2(\omega)) < 2\pi$ ). Therefore we suggest an additional condition

$$r_2(\omega) = r_1^*(\omega) \quad (3)$$

which fulfills the phase balance condition for evanescent waves at the mirrors. This leads to the Fabry-Perot resonance condition for evanescent waves

$$r_1(\omega)r_1^*(\omega)e^{-2\text{Im}k_z d} = 1 \quad (4)$$

We emphasize that phase balance occurs since  $\arg(r_1(\omega)r_1^*(\omega)e^{2ik_z d}) = 0$  and amplitude balance arises since  $|r_1(\omega)r_1^*(\omega)e^{-2\text{Im}k_z d}| = |r_1(\omega)|^2 e^{-2\text{Im}k_z d}$  can be unity when the exponential decay ( $e^{-2\text{Im}k_z d}$ ) is compensated by the enhancement ( $|r(\omega)| > 1$ ) due to evanescent coupling with surface waves.

The complex conjugation of the reflection coefficient ( $r^*(\omega)$ ) for evanescent wave Fabry-Perot resonances can be obtained by considering the negative frequency counterpart ( $r(-\omega)$ ) since the reality of fields [3] requires  $r(-\omega) = r^*(\omega)$ . Thus the problem of achieving such a resonance reduces to transforming the reflection from the second mirror into the negative frequency reflection coefficient of the first mirror  $r_2(\omega) = r_1(-\omega)$ . This can be achieved by setting two plates made of the same material in relative motion. This configuration of moving identical Fabry-Perot

plates is shown in Fig. 2 where one plate is moving at a constant velocity parallel to its surface. We assume the  $z$  axis is normal to the plates' surfaces and the motion is along the  $x$ -axis.

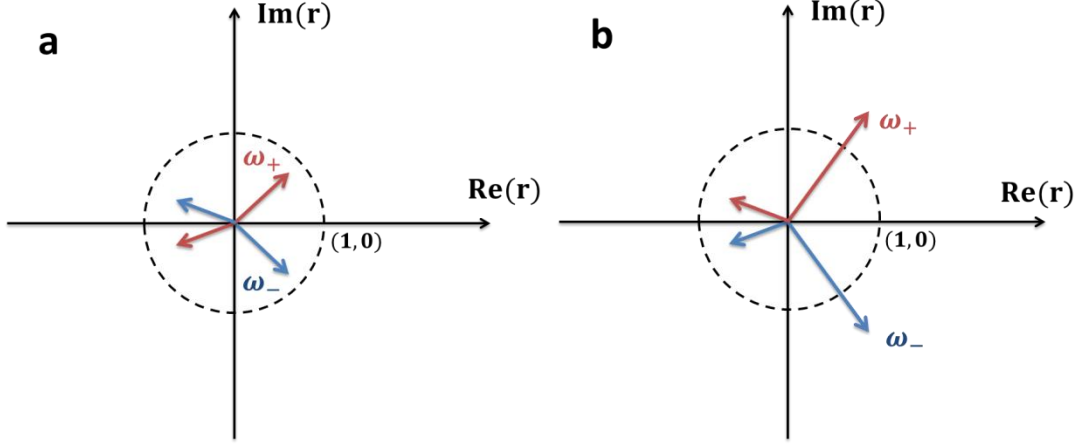


Figure 1. Complex reflection coefficients in passive media for positive (red) and negative frequencies (blue) **(a)** For propagating waves, the magnitude of the reflection coefficient should be smaller than one but there is no restriction on the phase. **(b)** For evanescent waves incident on a medium, the direction of energy tunneling is fixed implying that  $r$  should be in the upper complex space (both red phasors in the figure lie in the upper half of the complex plane). The magnitude  $|r|$  can be larger than one especially at surface wave resonances. We also illustrate the reflection coefficients for negative frequency propagating and evanescent waves which are complex conjugates of their positive frequency counterpart (blue phasors). Note that for evanescent waves,  $r(\omega)r(-\omega)$  can be a real number larger than one.

We now analyze the nature of the resonant modes within this gap. Consider an incident plane wave in vacuum given by  $e^{i(\vec{k}\cdot\vec{r}-\omega t)}$  on a moving interface. We consider the lateral wavevector  $(k_x, k_y)$  along the non-relativistic moving direction ( $V/c \ll 1$  and  $k_y = 0$ ) and provide the generalized approach in the Supplementary Information. The frequency of the wave in the frame co-moving at a constant velocity  $V$  along the  $x$  axis is Doppler shifted [2] to  $\omega' = \omega - k_x V$ . The dispersion relation of light in vacuum requires the wavevector along the interface for propagating waves to be smaller than the free space wavevector  $k_x < k_0$  where  $k_0 = \omega/c$ . This implies that the shifted frequency is always positive i.e.  $\omega|_{k_0} = \omega - k_x^{\max} V = \omega(1 - V/c) > 0$  since  $V < c$ . However, the wavevector of evanescent waves is necessarily larger than the free space

wavevector. This can lead to a negative Doppler shifted frequency in the near-field  $\omega' = \omega - k_x V < 0$  when  $k_x > \omega/V$ .

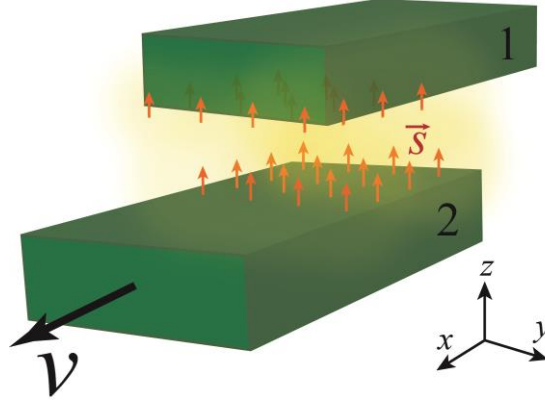


Figure 2. Singular Fabry-Perot (FP) resonance of evanescent waves can be achieved by setting the FP plates in relative motion. Plate 1 is stationary while plate 2 is moving at a constant velocity  $V$  along the  $x$  direction. The rest frame of plate 1 and plate 2 are denoted by lab frame and co-moving frame, respectively. The reflection coefficients and the distance can lead to a perfect balance of both phase and amplitude which cannot occur for propagating waves.

We therefore realize that an evanescent wave with frequency  $\omega$  incident on the stationary plate 1 will appear Doppler shifted to  $-\omega$  for the moving plate 2 when  $-\omega = \omega - k_x V$ . Thus evanescent waves with the wavevector

$$k_x^{PB} = 2 \frac{\omega}{V} \quad (5)$$

will bounce off the stationary first mirror with reflection coefficient  $r_1(\omega)$  but reflect off the second identical but moving mirror with coefficient  $r_1(-\omega)$ . This is because the reflection from a transversely moving plate does not alter the incident frequencies and can be expressed as the standard Fresnel reflection from a stationary plate with a Doppler shifted frequency (see Supplementary Information). We call this the phase balance wavevector. Using the near-field quasi-static approximation, the singular resonance condition gives  $|r_p|^2 e^{-4\omega d/V} = 1$ , so that

$$d^{AB} = \frac{V}{2\omega} \ln |r_p(\omega)|, \quad (6)$$

which is only possible when the reflection coefficient of p-polarized waves satisfies  $|r_p| > 1$  (see Supplementary Information). The phase balance (PB) and amplitude balance (AB) condition together can achieve the singular Fabry-Perot condition for evanescent waves. We emphasize that this condition holds true in the relativistic case as well leading to a singular resonant condition in spite of the presence of material dispersion and absorption (see Supplementary Information).

### Excitation of the singular resonance

Coupling energy from the far-field into near-field to excite the singular resonant mode becomes increasingly inefficient as the spectral width of the mode decreases. However, we now show that evanescent wave Fabry-Perot modes with vanishing spectral width can be spontaneously excited between moving bodies without the need for any external optical excitation. Near-field plates at different temperatures exchange thermal energy through excitation of allowed evanescent gap modes. However, even if we consider the temperature  $T$  of the identical plates to be the same, the Bose-Einstein distribution [4] of thermally excited modes  $n(\omega, T) = 1 / (e^{\hbar\omega/k_B T} - 1)$  within the moving plate will be Doppler shifted from the stationary plate. This drives an interesting photon exchange between the plates through the singular resonance.

For elucidation, we consider the zero temperature limit and analyze the photon exchange between the plates which is governed by two important factors: the emissivity/absorptivity and occupation of modes  $n(\omega)|_{T \rightarrow 0}$  in the plates [5–7]. For the stationary plate, there is no photon emission ( $N_1 = 0$ ) irrespective of the frequency of the modes. This is because the occupation number  $n(\omega)|_{T \rightarrow 0}$  is zero for all modes which necessarily have positive frequencies in the rest frame. However, the occupation of modes in the moving plate, which have to be evaluated in the co-moving frame, can be non-zero specifically for those modes which have negative Doppler shifted frequencies. The Bose-Einstein distribution gives  $n(\omega') = -1$  for  $\omega' < 0$ . We emphasize that this negative occupation is indicative of an excitation akin to population inversion made possible by the energy of motion. Such Doppler shifted negative frequency modes are evanescent in the gap and are emitted by the moving plate at a rate  $N_2 = 2 \text{Im}(r_2(\omega))n(\omega')|_{T \rightarrow 0}$  [7]. Here, the prefactor to the occupation probability of negative frequency modes corresponds to their near-

field emissivity, proportional to the evanescent wave Poynting vector ( $S_z \propto \text{Im}(r_2(\omega))$ ). The reflection coefficient  $r_2(\omega)$  is calculated in the lab frame, and the frequency in the occupation number should be that in the co-moving frame, the real frequency perceived by the moving plate. Note the photon emission rate  $N_2$  is greater than zero even though the occupation probability of modes within the moving plate is negative. This arises since the near-field emissivity ( $2\text{Im}(r_2(\omega))$ ) is negative for negative frequency evanescent wave modes, a phenomenon explained by the stark contrast between the Poynting vector directions for positive frequencies and negative frequencies (evanescent waves with  $k_x > \omega/V$ ). Since  $r(-\omega) = r^*(\omega)$ , we see that the Poynting vector of tunneling negative frequency waves  $S_z \propto \text{Im}(r)$  is opposite to that of positive frequency waves (Fig. 2). We thus note that as opposed to the conventional case of light tunneling into a medium, the negative frequency evanescent modes supported by a moving medium can tunnel out of it (Fig. 2). These photons will subsequently be absorbed by the stationary plate. The near-field absorptivity of the stationary plate is  $2\text{Im}[r_1(\omega)]$ , obtained by generalizing Kirchoff's law of thermal radiation to the near-field [8].

The total number of photons emitted by moving plate and then absorbed by the stationary plate is [7]

$$N(\omega, k_x) = \frac{2\text{Im}[r_1(\omega)] |e^{ik_z d}|^2 2\text{Im}[r_2(\omega)] n(\omega')}{|1 - r_1 r_2 e^{2ik_z d}|^2}, \quad (7)$$

where  $r_1$  and  $r_2$  are reflection coefficients for plate 1 and 2 evaluated in lab frame, the factor  $|e^{ik_z d}|^2$  accounts for the propagating decay of the photon between the two plates while  $1/|1 - r_1 r_2 e^{2ik_z d}|^2$  is for the multi-reflection between the plates. The singular Fabry-Perot resonance of evanescent waves leads to the divergence of this multi-reflection factor for the phase balance wavevector and amplitude balance distance.

To analyze the nature of the excited evanescent wave resonance in a practical scenario, we consider two identical metallic plates moving relative to each other at non-relativistic speeds. The moving velocity is bounded by the phonon velocity of the medium [9], typically in the order

of  $10^4$  m/s, thus  $\beta = V/c \ll 1$ . The plates are separated by a small gap to allow for interaction through large wavevector evanescent waves, necessary to achieve Doppler shifted negative frequencies in the co-moving frame. Since phase balance wavevector  $k_x^{PB}$  ( $2k_0/\beta$ ) is much larger than  $k_0$ , the reflection coefficient for p-polarized waves can be approximated by  $r_p(\omega) = (\varepsilon(\omega) - 1) / (\varepsilon(\omega) + 1)$ . When  $\text{Re}(\varepsilon(\omega)) = -1$ , there occurs a pole of the reflection coefficient corresponding to the surface wave resonance. The amplitude enhancement of an evanescent wave has a maximum at this surface wave resonance  $\omega_{SWR}$ , leading to the critical distance

$$d_0 = \frac{V}{2\omega_{SWR}} \ln |r_p(\omega_{SWR})|. \quad (8)$$

This expression shows that the amplitude balance condition for the singular FP resonance can be achieved by coupling to a surface wave resonance.

At the surface wave resonance, the magnitude of reflection coefficient  $|r_p|$  is bounded by the loss of the material. Realistic estimates for  $|r_p|$  is in the order of 10 and if the plate velocity is  $10^4$  m/s, the operating frequency  $\omega_{SWR}$  should be in the order of  $10^{12}$  Hz to give a critical distance in the order of 10 nm. Thus we need materials with low plasma frequency in the THz region to observe the singular Fabry-Perot resonance of evanescent waves. The possible options are phonon-polaritonic polar dielectrics, degenerately doped semiconductors [10] or graphene [11]. Here we consider a Drude metal with frequency dependent permittivity given by  $\varepsilon(\omega) = 1 - \omega_p^2 / (\omega^2 + i\Gamma\omega)$  with  $\omega_p = 3 \times 10^{12}$  Hz and  $\Gamma = 0.01\omega_p$ . The surface wave resonance frequency for this material is  $2.12 \times 10^{12}$  Hz and at the velocity of  $10^4$  m/s, the critical distance  $d_0$  that satisfies the singular resonance condition is close to 10 nm.

In Fig. 3, we plot the spectrum of photons exchanged according to their frequency and wavevector in the lab frame. For a distance  $d_1$  which is away from the singular Fabry-Perot Resonance condition of evanescent waves, we see two distinct bright regions in  $\omega - k$  space through which photons are spontaneously exchanged between the two plates. The vertical region corresponds to the surface wave resonance (SWR) frequency of the stationary plate where all

wavevectors are excited like in a conventional surface wave resonance. The curved region corresponds to the surface wave resonance frequency of the moving plate however the frequency is Doppler shifted and the region is curved instead of being a straight line.

As the plates are moved closer to the singular FP resonance condition ( $d \rightarrow d_0$ ), a fundamentally new mechanism of photon exchange emerges. This is evident from Fig. 3b where photons with the phase balance wavevector completely dominate the interaction. Note that this occurs when the frequencies in the co-moving frame and lab frame are equal and opposite, the condition for singular amplitude and phase balance. Indeed, the multiple scattering term  $1 - r_1 r_2 e^{2ik_z d}$  in equation 7, vanishes giving rise to an infinitely large number of photons exchanged.

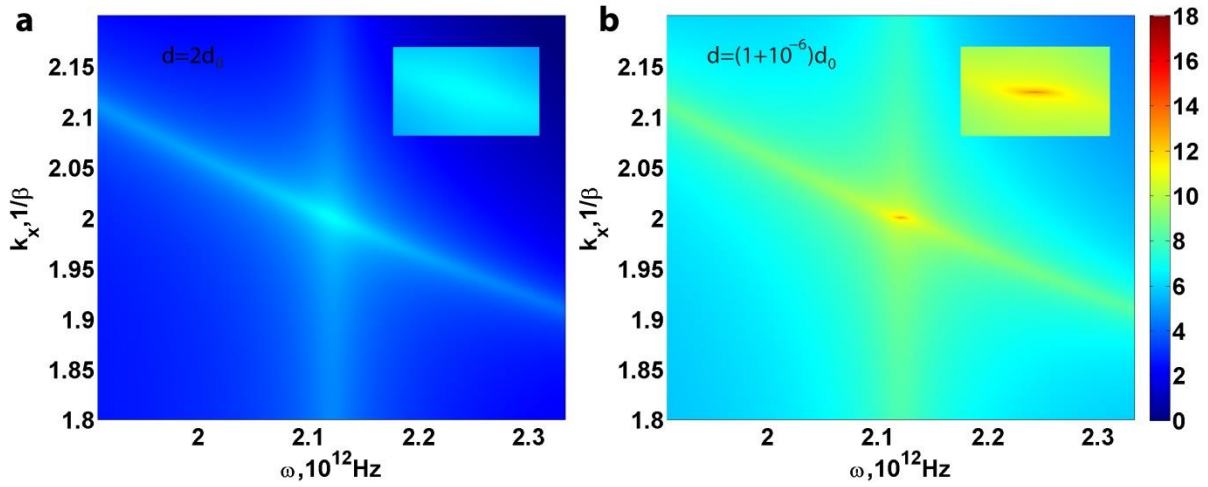


Figure 3. Contribution to exchanged photon number resolved by frequency and lateral wavevector  $k_x$  (normalized to free space wavevector) at (a)  $d=2d_0$  and (B)  $d \rightarrow d_0$ . In both (A) and (b), we see two bright curves, both of which are due to surface wave resonances. The vertical one comes from SWR at the interface of the stationary plate and vacuum while the other one is due to SWR at the interface of the moving plate and vacuum. These two bright curves join at the phase balance wavevector when the Doppler shifted SWR frequency in the co-moving frame is opposite to the SWR frequency in the lab frame. In (a), at a distance away from  $d_0$ , the singular resonance condition is far from being satisfied. However, the bright curves remain due to the SWR at the two interfaces. In (b), the red bright point is due to the singular resonance that arises since the amplitude balance condition is satisfied when  $d \rightarrow d_0$  and  $k_x = 2/\beta$ . This leads to giant photon exchange between moving plates at the phase and amplitude balance condition. The insets give the zoom in plots near the intersection of the two SWRs to emphasize the dramatic increase in the photon exchange due to the singular FP resonance of evanescent waves.

### Divergent force between Fabry-Perot mirrors

Once excited, Fabry-Perot modes exert light pressure [12] on the mirrors. In the case of moving mirrors we expect both a lateral and transverse force. We focus here on the observable force on the plates in a direction opposite to the motion known as quantum friction [7,9,13–19] which arises due to momentum carried by the photons exchanged between the plates. This dispersive force, i.e., the momentum transfer between the two plates [7], is the product of the total number of photons exchanged (equation 7) and the momentum of a single photon  $\hbar k_x$  ( $\hbar$  is the Planck constant divided by  $2\pi$ )  $f_x(\omega, k_x) = \hbar k_x N(\omega, k_x)$ . The net force  $F$  can be achieved by integrating all possible partial waves (see Supplementary Information).

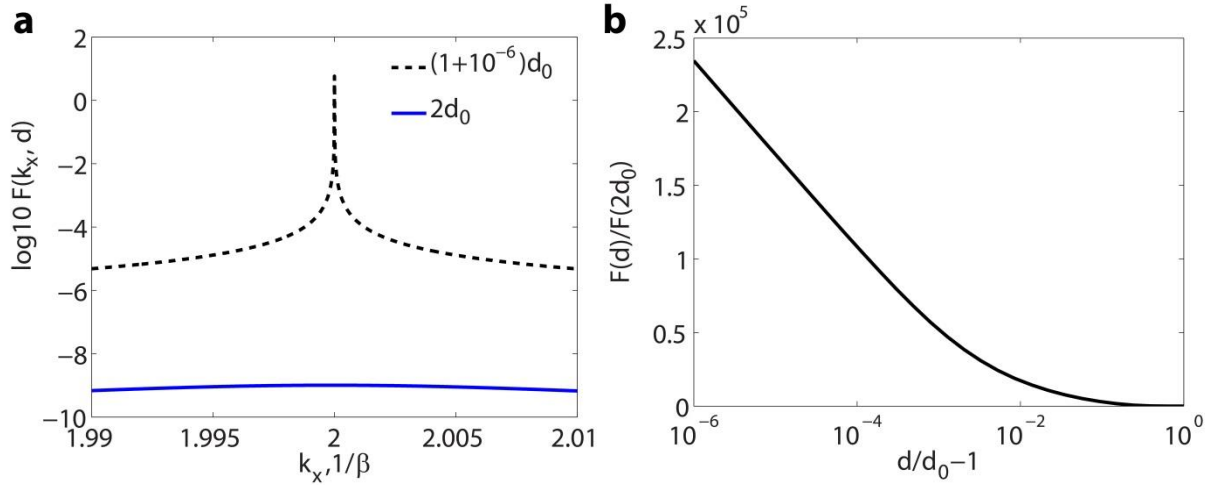


Figure 4. Quantum frictional force on the FP plates (a) resolved by the wavevector  $k_x$  at  $d=d_0^+$  and  $d=2d_0$ . A major contribution to the force arises from modes at the perfect phase balance wavevector. However, at  $2d_0$ , the amplitude of friction is significantly smaller. (b) The distance dependence of friction at distances near  $d_0$ . The x axis is in  $(d/d_0-1)$  and log scale. We clearly see a linear increasing behavior as  $d$  approaches  $d_0$ . This is consistent with the theoretical scaling law which predicts a logarithmic divergence of the quantum electrodynamic frictional force in the ideal limit.

In Fig. 4a, we plot the spectrum of the quantum friction force resolved according to the wavevector for various distances of the plates. The largest contribution to the force is due to the Fabry-Perot resonance of evanescent waves. This can be interpreted as a perfect coupling of positive and negative frequencies in the near-field. In fact, it is interesting to note that this quantum frictional force actually diverges whenever the plates can support the singular

resonance. When the distance  $d$  approaches the critical distance  $d_0$ , the quantum friction  $F$  scales as  $\ln[d_0/(d-d_0)]$  (see Supplementary Information). We plot the friction vs. distance in Fig. 4b to verify the theoretical predictions. The x-axis is  $(d/d_0 - 1)$  in log scale. We clearly see that the friction increases linearly as a function of  $\ln[d_0/(d-d_0)]$  when  $d$  approaches  $d_0$ , consistent with the theoretical scaling law which predicts a divergence.

We emphasize that singular resonances introduced in this paper require a pole of the scattering matrix to lie on the real axis which is precluded by the requirement of an infinite energy supply for maintaining relative motion. Even though losses and dispersion are not a fundamental impediment to the FP resonance, the presence of nonlinear responses at huge energy flux and non-local effects in the dielectric permittivity at close proximity [20] will prevent any such divergences in experiment. However, the giant enhancement in the quantum friction force due the resonance predicted in the paper can be ascertained either with THz surface waves in doped semiconductors [10], phonon-polaritonic polar dielectrics or graphene [11].

## Conclusion

In summary, we have introduced a singular resonance supported by moving media. The resonance arises due to the coupling of positive and negative frequency evanescent waves and leads to a spontaneous exchange of a large number of photons between the moving bodies. The non-contact frictional force mediated by a nanoscale vacuum gap can diverge due to the existence of this evanescent wave Fabry-Perot resonance. Negative frequency effects lie at the heart of multiple phenomena from the dynamic Casimir force [7,21] and Zel'dovich super-radiance [22,23] to Hawking radiation [24] and Unruh effect [25,26]. Experiments with artificial media (metamaterials) and nanoscale motors, torsional resonators and nanomechanical systems can manifest such resonances leading to a deeper understanding of the Lorentz invariance of vacuum fluctuations [27,28].

## Acknowledgments:

We acknowledge funding from National Science and Engineering Research Council of Canada and Alberta Innovates Technology Futures.

## References:

1. M. Wolf and E. Born, *Principles of Optics: Electromagnetic Theory of Propagation, Interference and Diffraction of Light* (Cambridge University Press, 1980).
2. J. A. Kong, *Electromagnetic Wave Theory* (Wiley New York, 1990), Vol. 2.
3. L. Landau, E. Lifshitz, and L. Pitaevskii, *Electrodynamics of Continuous Media* (Pergamon Press, Oxford, 1984).
4. L. Landau, E. Lifshitz, and L. Pitaevskii, *Statistical Physics, Part. I* (Pergamon Press, Oxford, 1980), Vol. 24.
5. J. B. Pendry, "Radiative exchange of heat between nanostructures," *J. Phys. Condens. Matter* **11**, 6621 (1999).
6. S.-A. Biehs, E. Rousseau, and J.-J. Greffet, "Mesoscopic Description of Radiative Heat Transfer at the Nanoscale," *Phys. Rev. Lett.* **105**, 234301 (2010).
7. M. F. Maghrebi, R. Golestanian, and M. Kardar, "Scattering approach to the dynamical Casimir effect," *Phys. Rev.* **87**, 025016 (2013).
8. S. Rytov, Y. A. Kravtsov, and V. Tatarskii, *Principles of Statistical Radiophysics. Vol. 3. Wave Propagation through Random Media* (Springer, Berlin, 1989).
9. J. B. Pendry, "Shearing the vacuum - quantum friction," *J. Phys. Condens. Matter* **9**, 10301 (1997).
10. R. Zhao, A. Manjavacas, F. J. Garc ía de Abajo, and J. B. Pendry, "Rotational Quantum Friction," *Phys. Rev. Lett.* **109**, 123604 (2012).
11. A. I. Volokitin and B. N. J. Persson, "Quantum Friction," *Phys. Rev. Lett.* **106**, 094502 (2011).
12. R. Loudon, "Theory of the radiation pressure on dielectric surfaces," *J. Mod. Opt.* **49**, 821–838 (2002).
13. E. V. Teodorovich, "On the Contribution of Macroscopic Van Der Waals Interactions to Frictional Force," *Proc. R. Soc. Lond. Math. Phys. Sci.* **362**, 71–77 (1978).
14. L. S. Levitov, "Van Der Waals' Friction," *EPL Eur. Lett.* **8**, 499 (1989).
15. G. Barton, "The Quantum Radiation from Mirrors Moving Sideways," *Ann. Phys.* **245**, 361–388 (1996).
16. J. B. Pendry, "Can sheared surfaces emit light?," *J. Mod. Opt.* **45**, 2389–2408 (1998).
17. A. I. Volokitin and B. N. J. Persson, "Theory of friction: the contribution from a fluctuating electromagnetic field," *J. Phys. Condens. Matter* **11**, 345 (1999).
18. A. I. Volokitin and B. N. J. Persson, "Theory of the interaction forces and the radiative heat transfer between moving bodies," *Phys. Rev. B* **78**, 155437 (2008).
19. T. G. Philbin and U. Leonhardt, "No quantum friction between uniformly moving plates," *New J. Phys.* **11**, 033035 (2009).
20. C. Cirac, R. T. Hill, J. J. Mock, Y. Urzhumov, A. I. Fernández-Dom ínguez, S. A. Maier, J. B. Pendry, A. Chilkoti, and D. R. Smith, "Probing the Ultimate Limits of Plasmonic Enhancement," *Science* **337**, 1072–1074 (2012).
21. G. T. Moore, "Quantum Theory of the Electromagnetic Field in a Variable-Length One-Dimensional Cavity," *J. Math. Phys.* **11**, 2679–2691 (1970).
22. Y. B. Zel'Dovich, "Generation of Waves by a Rotating Body," *Sov. J. Exp. Theor. Phys. Lett.* **14**, 180 (1971).
23. M. F. Maghrebi, R. L. Jaffe, and M. Kardar, "Spontaneous Emission by Rotating Objects: A Scattering Approach," *Phys. Rev. Lett.* **108**, 230403 (2012).

24. S. W. Hawking, "Black hole explosions?," *Nature* **248**, 30–31 (1974).
25. W. G. Unruh, "Notes on black-hole evaporation," *Phys. Rev.* **14**, 870–892 (1976).
26. P. D. Nation, J. R. Johansson, M. P. Blencowe, and F. Nori, "Colloquium: Stimulating uncertainty: Amplifying the quantum vacuum with superconducting circuits," *Rev. Mod. Phys.* **84**, 1–24 (2012).
27. P. W. Milonni, *The Quantum Vacuum: An Introduction to Quantum Electrodynamics* (Academic Press, 1994).
28. T. H. Boyer, "Derivation of the Blackbody Radiation Spectrum without Quantum Assumptions," *Phys. Rev.* **182**, 1374–1383 (1969).

# Supplementary Information for “Singular evanescent wave resonances”

Yu Guo and Zubin Jacob\*

\*[zjacob@ualberta.ca](mailto:zjacob@ualberta.ca)

## Derivation of Poynting vector

A p-polarized incident plane wave,  $H_i = \hat{y}e^{i(k_x x + k_y y + k_z z - \omega t)}$ , shines on the interface in x-y plane between vacuum and a plate. Here  $k_x$  and  $k_y$  are real,  $k_z = \sqrt{(\omega/c)^2 - k_x^2 - k_y^2}$ ,  $k_z$  is real for propagating waves (PWs) while imaginary for evanescent waves (EWs). Assuming that the reflection coefficient is  $r$ , the reflected wave will be  $H_r = \hat{y}r e^{i(k_x x + k_y y - k_z z - \omega t)}$ . The electric fields lying along the interface are  $E_{ix} = \hat{x} \frac{k_z}{\omega \mu_0} e^{i(k_x x + k_y y + k_z z - \omega t)}$ ,  $E_{rx} = \hat{x} \frac{-k_z r}{\omega \mu_0} e^{i(k_x x + k_y y - k_z z - \omega t)}$ . Thus the Poynting vector [1] along the normal direction is

$$S_z = \frac{1}{2} \text{Re}(E \times H^*)_z = \begin{cases} \frac{k_z}{2\omega\mu_0} (1 - |r|^2), & \text{PWs} \\ \frac{|k_z|}{2\omega\mu_0} 2 \text{Im}(r), & \text{EWs} \end{cases} \quad (\text{S1})$$

Then the energy absorbed by the plate is proportional to  $1 - |r|^2$  for PWs and  $2 \text{Im}(r)$  for EWs. For a stationary passive medium,  $S_z$  must be positive so  $1 - |r|^2 > 0$  for PWs and  $\text{Im}(r) > 0$  for EWs. It is worthwhile noting that  $1 - |r|^2$  is the far field emissivity related to the absorption of propagating waves and  $2 \text{Im}(r)$  can be physically interpreted as the near field emissivity [2–4] in the photon emission process. The above result has been utilized throughout the manuscript to understand the tunneling of evanescent waves emanating from the moving mirror.

## On the reality of fields

The key condition for the Fabry-Perot resonance of evanescent waves is obtained by the complex conjugation of the reflection coefficients. In the main text we have argued that this can be achieved using the negative frequency counterpart of the reflection coefficient. This result relies on the condition for the reality of the fields [5]. In Fourier space, the electric fields are expressed as

$$E(r, t) = \int u(\omega, k_x, k_y, z) e^{i(k_x x + k_y y - \omega t)} dk_x dk_y d\omega. \quad (\text{S2})$$

In view of the reality of  $E(r, t)$ ,

$$u(\omega, k_x, k_y, z) = u^*(-\omega, -k_x, -k_y, z). \quad (\text{S3})$$

This is valid for both the incident waves and the reflected waves. For reflections from a stationary plate with the in plane wavevectors  $(k_x, k_y)$  conserved,

$$r(\omega, k_x, k_y) = r^*(-\omega, -k_x, -k_y). \quad (\text{S4})$$

In this work, we assume the reflection coefficients are written for isotropic media so that

$$r(\omega, k_x, k_y) = r(\omega, -k_x, -k_y). \quad (\text{S5})$$

Thus for reflection from a stationary plate, we have

$$r(\omega, k_x, k_y) = r^*(-\omega, k_x, k_y). \quad (\text{S6})$$

## The scattering matrix of a moving plate with polarization mixing

In the main text, for simplicity, we have assumed non-relativistic velocities and no mixing of polarizations. However, here we generalize our approach and show that the central result related to the singular resonance of evanescent waves persists even in the relativistic limit.

We start from the Lorentz transformation [1],

$$\begin{bmatrix} E' \\ cB' \end{bmatrix} = \gamma \begin{bmatrix} \vec{\alpha}^{-1} & \vec{\beta} \\ -\vec{\beta} & \vec{\alpha}^{-1} \end{bmatrix} \begin{bmatrix} E \\ cB \end{bmatrix}, \quad (\text{S7})$$

where

$$\vec{\alpha}^{-1} = \begin{bmatrix} 1/\gamma & 0 & 0 \\ 0 & 1 & 0 \\ 0 & 0 & 1 \end{bmatrix}, \vec{\beta} = \begin{bmatrix} 0 & 0 & 0 \\ 0 & 0 & -\beta \\ 0 & \beta & 0 \end{bmatrix}, \quad (\text{S8})$$

with  $\beta = V/c$ ,  $\gamma = 1/\sqrt{1-\beta^2}$ .

The electric fields are transformed by

$$\vec{E}' = \gamma(\vec{\alpha}^{-1}\vec{E} + \vec{\beta}cB). \quad (\text{S9})$$

For plane waves with phase  $e^{i(k_x x + k_y y + k_z z - \omega t)}$ ,

$$cB = \frac{c}{\omega} \vec{k} \times \vec{E} = \frac{c}{\omega} \begin{bmatrix} 0 & -k_z & k_y \\ k_z & 0 & -k_x \\ -k_y & k_x & 0 \end{bmatrix} \vec{E} = \frac{c}{\omega} \vec{k} \vec{E}. \quad (\text{S10})$$

For the frequency and wavevector, the Lorentz transformation gives [1],

$$k'_x = \gamma(k_x - \beta k_0), \quad (\text{S11})$$

$$\omega' = \gamma(\omega - k_x V), \quad (\text{S12})$$

while  $k_y$  and  $k_z$  remain unchanged.

We first transform the incident field to the co-moving frame,

$$\vec{E}' = \gamma(\vec{\alpha}^{-1} + \frac{c}{\omega} \vec{\beta} \vec{k}) \vec{E}. \quad (\text{S13})$$

The reflected fields in the co-moving frame are

$$\vec{E}'_r = (r'_s \hat{s}'_- \hat{s}'_+ + r'_p \hat{p}'_- \hat{p}'_+) \vec{E}'. \quad (\text{S14})$$

Here  $\hat{s}'_+ = \hat{s}'_- = (k'_y, -k'_x, 0)/k'_\rho$  are the unit vectors of upward and downward s-polarized waves,

$\hat{p}'_+ = [-k'_x k'_z \quad -k'_y k'_z \quad (k'_\rho)^2]/k'_0 k'_\rho$ ,  $\hat{p}'_- = [k'_x k'_z \quad k'_y k'_z \quad (k'_\rho)^2]/k'_0 k'_\rho$  are the unit vectors of

forward and downward p-polarized waves, respectively, where  $k'_0 = \omega'/c$ ,  $k'_\rho = \sqrt{(k'_x)^2 + (k'_y)^2}$ .

$r'_s$  and  $r'_p$  are the standard Fresnel reflection coefficient of s- and p-polarized waves in the co-moving frame, respectively.

Next we transform the reflected field to the lab frame,

$$E_r = \gamma(\tilde{\alpha}^{-1} + \frac{c}{\omega'} \tilde{\beta}' \tilde{k}') E_r'. \quad (\text{S15})$$

Here

$$\tilde{\beta}' = \begin{bmatrix} 0 & 0 & 0 \\ 0 & 0 & \beta \\ 0 & -\beta & 0 \end{bmatrix} = -\tilde{\beta}, \tilde{k}' = \frac{c}{\omega'} \begin{bmatrix} 0 & -k'_z & k'_y \\ k'_z & 0 & -k'_x \\ -k'_y & k'_x & 0 \end{bmatrix}. \quad (\text{S16})$$

Thus  $E_r = RE$  where the reflection operator is given by

$$R = \gamma(\tilde{\alpha}^{-1} + \frac{c}{\omega'} \tilde{\beta}' \tilde{k}') (r'_s \hat{s}'_+ \hat{s}'_+ + r'_p \hat{p}'_- \hat{p}'_+) \gamma(\tilde{\alpha}^{-1} + \frac{c}{\omega'} \tilde{\beta}' \tilde{k}'). \quad (\text{S17})$$

For an alternative derivation of this reflection operator, see Ref. [6].

Now the reflection operator is written in a 3 by 3 matrix. The 2 by 2 reflection matrix is defined by

$$r_{\lambda\mu} = \hat{e}_\lambda^- R \hat{e}_\mu^+, \quad (\text{S18})$$

where  $r_{\lambda\mu}$  are the reflection coefficients for an incident wave with polarization  $\mu$  to be reflected as a wave with polarization  $\lambda$ .  $\hat{e}_s^\pm = [k_y \quad -k_x \quad 0]/k_\rho$ ,  $\hat{e}_p^\pm = [\mp k_x k_z \quad \mp k_y k_z \quad k_\rho^2]/k_0 k_\rho$  ( $k_0 = \omega/c$ ,  $k_\rho = \sqrt{k_x^2 + k_y^2}$ ) are the unit vector of s- and p-polarized waves in the vacuum, respectively. As before, the plus sign in the superscript of  $\hat{e}$  denotes forward waves (incident waves) and the minus sign for downward waves (reflected waves). After some lengthy but straightforward calculations, the scattering matrix of the moving plate  $r_{\lambda\mu}$  is found to be

$$r_{\lambda\mu} = \begin{bmatrix} r_{ss} & r_{sp} \\ r_{ps} & r_{pp} \end{bmatrix} = B \begin{bmatrix} r'_s & \\ & r'_p \end{bmatrix} A. \quad (\text{S19})$$

Here the matrix elements  $A_{11} = A_{22} = \gamma k'_0 (k_\rho^2 - \beta k_0 k_x) / k_0 k'_\rho k_\rho$ ,  $A_{12} = -A_{21} = \gamma k'_0 (-\beta k_y k_z) / k_0 k'_\rho k_\rho$ ,  $B_{11} = B_{22} = \gamma k_0 (k_\rho^2 - \beta k_0 k_x) / k'_0 k'_\rho k_\rho$ ,  $B_{12} = -B_{21} = \gamma k_0 (-\beta k_y k_z) / k'_0 k'_\rho k_\rho$ . The reflection coefficients are

$$r_{ss} = r'_s \gamma^2 (k_\rho^2 - \beta k_0 k_x)^2 / (k'_\rho k'_\rho)^2 - r'_p \gamma^2 (\beta k_y k_z)^2 / (k'_\rho k'_\rho)^2, \quad (\text{S20})$$

$$r_{sp} = -(r'_s + r'_p) \gamma^2 (k_\rho^2 - \beta k_0 k_x) \beta k_y k_z / (k'_\rho k'_\rho)^2, \quad (\text{S21})$$

$$r_{ps} = (r'_s + r'_p) \gamma^2 (k_\rho^2 - \beta k_0 k_x) \beta k_y k_z / (k'_\rho k'_\rho)^2 = -r_{sp}, \quad (\text{S22})$$

$$r_{pp} = r'_p \gamma^2 (k_\rho^2 - \beta k_0 k_x)^2 / (k'_\rho k'_\rho)^2 - r'_s \gamma^2 (\beta k_y k_z)^2 / (k'_\rho k'_\rho)^2. \quad (\text{S23})$$

Generally speaking, the reflected waves of p-polarized waves will have s-polarized waves component, and vice versa. This is called polarization mixing. Note polarization mixing will not be a big effect at non-relativistic velocity due to the factor  $\beta$  in both  $r_{sp}$  and  $r_{ps}$ .

However, for  $k_y = 0$ , we have

$$r_{ss}(\omega, k_x) = r'_s(\omega', k'_x), \quad (\text{S24})$$

$$r_{pp}(\omega, k_x) = r'_p(\omega', k'_x), \quad (\text{S25})$$

and

$$r_{sp} = r_{ps} = 0. \quad (\text{S26})$$

This means, when  $k_y = 0$ , polarization mixing disappears regardless of the velocity. The reflection from a moving plate can be expressed as the standard Fresnel reflection from a stationary plate with a Doppler shifted frequency and wavevector. In the main text, we only consider the p-polarized waves with  $k_y = 0$ , thus  $r_p(\omega, k_x) = r'_p(\omega', k'_x)$ . The polarization of the wave does not change on reflection.

At the relativistic phase balance wavevector (set  $\omega' = -\omega$  in Eq. (S12))

$$k_x = (1 + \frac{1}{\gamma}) \frac{\omega}{V}, \quad (\text{S27})$$

we have

$$\omega' = -\omega, k'_x = k_x. \quad (\text{S28})$$

Thus  $r_p(\omega, k_x) = r'_p(-\omega, k_x)$ . Here  $r'_p$  is reflection from a stationary plate in the co-moving frame, so  $r_p(\omega, k_x) = (r'_p(\omega, k_x))^*$ , which is the complex conjugate of the reflection coefficient from the

stationary plate in the lab frame. In this sense, we achieve  $r_2 = r_1^*$  at the phase balance wavevector.

The expression for the Poynting vector is also valid for a moving plate since it only depends on the reflection coefficients. At the lab frame, we only consider positive frequency, namely  $\omega > 0$ . When the Doppler shifted frequency  $\omega' < 0$ ,  $\text{Im}(r)$  will be negative, resulting in a negative Poynting vector. Thus essentially we extract energy out from the moving plate.

### Approximation of the reflection coefficients

The moving velocity is bounded by the phonon velocity of the medium, typically in the order of  $10^4$  m/s, thus  $\beta$  is very small in the order of  $10^{-4}$ . As  $k_x$  is very large to achieve negative frequency ( $k_x > k_0/\beta$ ), the reflection coefficients can be evaluated by the high-k approximation.

For a stationary plate with a very large  $k_x$ ,

$$r_s = \frac{\varepsilon - 1}{4(k_\rho/k_0)^2}, \quad (\text{S29})$$

and

$$r_p = \frac{\varepsilon - 1}{\varepsilon + 1}. \quad (\text{S30})$$

The reflection coefficient for s-polarized waves is negligibly small, while  $|r_p|$  has a resonance at  $\text{Re}(\varepsilon) = -1$ , which is the surface waves resonance condition.

To compensate the propagating decay of evanescent waves inside the vacuum gap,  $|r_p|$  should be larger than 1, thus implying  $\text{Re}(\varepsilon) < 0$ . This means the structure needs to work in the frequency spectrum where the materials are metallic.

## Full theory for photon exchange

In the main text, we have argued that the spontaneously occurring photon exchange between the plates diverges due to the existence of the singular resonance condition. Here for completeness, we provide the complete relativistic theory of the photon exchange and relate it to quantum friction to emphasize how the phase balance and amplitude balance condition enters in the analysis.

In the main text, we have assumed that  $k_y = 0$  to avoid polarization mixing of waves. Thus we can deal with p- and s-polarized waves separately. The scattering matrix, i.e., the reflection matrix, will be diagonal and can be handled as scalars. However, if  $k_y \neq 0$ , the scattering matrix  $r_{\lambda\mu}$  of the moving plate will have non-diagonal terms, i.e., polarization mixing terms. Therefore we need the full theory with polarization mixing and relativistic velocity taken into account to describe the photon exchange picture.

The spontaneous emission rate from a moving plate at constant velocity is [4,7–9]

$$\text{Tr}(1 - SS^\dagger)n(\omega', T) \quad (\text{S31})$$

for propagating waves and

$$\text{Tr}(i(S^\dagger - S))n(\omega', T) \quad (\text{S32})$$

for evanescent waves. Here,  $S$  is the classical scattering matrix evaluated in the lab frame,  $\omega'$  is the frequency in the plate's rest frame,  $n(\omega', T)$  is the Bose-Einstein occupation number [10] in the co-moving frame, ' $\dagger$ ' denotes Hermitian conjugate, 'Tr' means taking the trace.  $(1 - SS^\dagger)$  and  $i(S^\dagger - S)$  can be also seen as the absorption rate of the incident waves by the plates.

Assuming  $U$  is the spontaneous emission (absorption) amplitude of the plate [4]. For propagating waves,  $UU^\dagger = 1 - SS^\dagger$ ; for evanescent waves,  $UU^\dagger = i(S^\dagger - S)$ . In the configuration of Fig. 2, the amplitude of photon emitted by plate 1 and then absorbed by the plate 2 is  $U_2 e^{ik_z d} U_1$ , where  $e^{ik_z d}$  accounts for the propagating with the vacuum gap. Taking the multi-reflection into account [4], the amplitude is

$$U_2(1 + e^{2ik_z d} R_1 R_2 + (e^{2ik_z d} R_1 R_2)^2 + \dots) e^{ik_z d} U_1 = U_2 \frac{e^{ik_z d}}{1 - R_1 R_2 e^{2ik_z d}} U_1. \quad (\text{S33})$$

With the Bose-Einstein occupation number  $n_1(\omega, T_1)$  of plate 1, the photon transfer rate from plate 1 to plate 2 is [8,9]

$$N_{1 \rightarrow 2} = \text{Tr} \left[ (U_2 \frac{e^{ik_z d}}{1 - R_1 R_2 e^{2ik_z d}} U_1) (U_2 \frac{e^{ik_z d}}{1 - R_1 R_2 e^{2ik_z d}} U_1)^\dagger \right] n_1(\omega, T_1). \quad (\text{S34})$$

Similarly, the photon transfer rate from plate 2 to plate 1 is

$$N_{2 \rightarrow 1} = \text{Tr} \left[ (U_1 \frac{e^{ik_z d}}{1 - R_2 R_1 e^{2ik_z d}} U_2) (U_1 \frac{e^{ik_z d}}{1 - R_2 R_1 e^{2ik_z d}} U_2)^\dagger \right] n_2(\omega', T_2). \quad (\text{S35})$$

It can be shown that

$$\begin{aligned} & \text{Tr} \left[ (U_2 \frac{e^{ik_z d}}{1 - R_1 R_2 e^{2ik_z d}} U_1) (U_2 \frac{e^{ik_z d}}{1 - R_1 R_2 e^{2ik_z d}} U_1)^\dagger \right] \\ &= \text{Tr} \left[ (U_1 \frac{e^{ik_z d}}{1 - R_2 R_1 e^{2ik_z d}} U_2) (U_1 \frac{e^{ik_z d}}{1 - R_2 R_1 e^{2ik_z d}} U_2)^\dagger \right]. \end{aligned} \quad (\text{S36})$$

The net photon exchanged rate should be  $N = N_{2 \rightarrow 1} - N_{1 \rightarrow 2}$ . One then finds that

$$N = \text{Tr} \left[ (1 - S_1^\dagger S_1) D (1 - S_2 S_2^\dagger) D^\dagger \right] (n_2(\omega', T_2) - n_1(\omega, T)) \quad (\text{S37})$$

for propagating waves, and

$$N = \text{Tr} \left[ (S_1 - S_1^\dagger) D (S_2^\dagger - S_2) D^\dagger \right] (n_2(\omega', T_2) - n_1(\omega, T)) \quad (\text{S38})$$

for evanescent waves, where  $D = \frac{e^{ik_z d}}{1 - R_2 R_1 e^{2ik_z d}}$ .

Here we are interested in  $T_1 = T_2 = 0\text{K}$ , under which condition  $n(\omega, T)$  vanishes for positive frequencies and equals  $-1$  for negative frequencies. In the lab frame, we only consider positive frequency photons, so essentially no photon emitted from plate 1. However, for the moving plate 2, the photon emission can be nonzero for negative Doppler shifted waves  $\omega' < 0$ , under the condition  $k_x > \omega/V$ . With the help of the scattering matrix and after some algebra, one can derive the expression for number of photon exchanged,

$$N(\omega, k_x, k_y) = -\frac{4}{|\Delta|^2} ((k_\rho^2 - \beta k_0 k_x)^2 + \beta^2 k_z^2 k_y^2) e^{-2\text{Im}(k_z)d} ((k_\rho^2 - \beta k_0 k_x)^2 \times \text{Im}(r_{1p}) \text{Im}(r'_{2p}) |D_{ss}|^2 - \beta^2 k_z^2 k_y^2 \text{Im}(r_{1p}) \text{Im}(r'_{2s}) |D_{sp}|^2 + (p \rightarrow s)) \quad (\text{S39})$$

Here  $k_\rho = \sqrt{k_x^2 + k_y^2}$ ,  $\beta = V/c$ ,  $\gamma = 1/\sqrt{1-\beta^2}$ ,  $k_0 = \omega/c$ ,  $k'_x = \gamma(k_x - \beta k_0)$ ,  $\omega' = \gamma(\omega - k_x V)$ ,  $k'_z = \sqrt{k_0^2 - k_\rho^2}$ ,  $D_{ss} = 1 - e^{2ik_z d} r_{1s} r'_{2s}$ ,  $D_{pp} = 1 - e^{2ik_z d} r_{1p} r'_{2p}$ ,  $D_{sp} = 1 + e^{2ik_z d} r_{1s} r'_{2p}$ ,  $D_{ps} = 1 + e^{2ik_z d} r_{1p} r'_{2s}$ ,  $\Delta = (k_\rho^2 - \beta k_0 k_x)^2 D_{ss} D_{pp} + \beta^2 k_z^2 k_y^2 D_{sp} D_{ps}$ . The symbol  $p \leftrightarrow s$  denotes the terms that can be gained by permuting the indexes p and s of preceding terms.  $r_{1(s,p)}$  are the reflection coefficients from the stationary plate,  $r'_{2(s,p)}$  are the reflection coefficients in the co-moving frame.  $\Delta$  is the denominator of the matrix  $(1 - R_2 R_1 e^{2ik_z d})^{-1}$ .

### Singular Resonance at relativistic velocity

In the main text, we have assumed a non-relativistic Lorentz transform and no polarization mixing. We then find the multi-reflection factor  $1 - r_1 r_2 e^{2ik_z d}$  is real at the phase balance wavevector, which can lead to singular resonance at proper chosen distance. Here we show that the singular resonance can exist in spite of relativistic effects and polarization mixing.

At the relativistic phase balance wavevector,  $k_x = (1 + 1/\gamma)\omega/V$ ,  $\omega' = -\omega$ ,  $k'_x = k_x$  (Eq. (S27) and (S28)). The transform make the frequency opposite and keep the wavevector unchanged, consistent with the invariance of the four dimensional momentum vector. Due to the reality of fields, the reflection coefficients in the co-moving frame at frequency  $-\omega$  are the complex conjugates of corresponding reflection coefficients in the lab frame at frequency  $\omega$ ,  $r'_{2(s,p)} = r_{1(s,p)}^*$ .

Thus  $D_{ss}$ ,  $D_{pp}$  are real and  $D_{sp} = D_{ps}^*$ , so that  $\Delta$  is real valued at the relativistic phase balance vector.

To be consistent with the case  $k_y = 0$ , we define the normalized  $\Delta_N$  rather than  $\Delta$  in Eq. (S39) as the multi-reflection factor,

$$\Delta_N = \frac{(k_\rho^2 - \beta k_0 k_x)^2 D_{ss} D_{pp} + \beta^2 k_z^2 k_y^2 D_{sp} D_{ps}}{(k_\rho^2 - \beta k_0 k_x)^2 + \beta^2 k_z^2 k_y^2}. \quad (\text{S40})$$

In the region  $\beta < 10^{-4}$ , since  $k_x > k_0/\beta$ , one has  $\beta^2 k_z^2 k_y^2 \ll (k_\rho^2 - \beta k_0 k_x)^2$  and  $D_{ss} \approx 1$ . Thus  $\Delta_N$  is well approximated by  $D_{pp}$ . At the phase balance wavevector  $k_x^{PB} = 2\omega/V$ ,  $D_{pp}(k_x^{PB}) = 1 - |r_p(\omega)|^2 e^{-4\omega d/V}$ , we can adjust the distance  $d$  to make it zero as long as  $|r_p| > 1$ . It is clear that  $D_{pp}$  has a local minimum at  $(\omega_{SWR}, k_x^{PB}, k_y = 0)$  due to the surface wave resonance of  $|r_p(\omega)|$ . That  $D_{pp}$  equals zero at this minimum leads to

$$d_0 = \frac{V}{2\omega_{SWR}} \ln |r_p(\omega_{SWR})|. \quad (\text{S41})$$

Thus we prove the singular resonance with an infinite quality factor exists in the presence of relativistic velocity and polarization mixing.

## Quantum friction

The dispersive force, i.e., the momentum transfer between the two plates [4], is the product of the total number of exchanged photons and the momentum of a single photon  $\hbar k_x$  ( $\hbar$  is the Planck constant divided by  $2\pi$ )

$$f_x(\omega, k_x, k_y) = \hbar k_x N(\omega, k_x, k_y). \quad (\text{S42})$$

We also note that the energy transfer between the two plates is the product of the total number of photons exchanged and the energy of a single photon  $\hbar\omega$ .

The net dispersive force can be achieved by integrating all possible partial waves  $\omega$ ,  $k_x$  and  $k_y$  [4] in the above Eq. (S42). Note that the frequency  $\omega$  should be positive and  $k_x > \omega/V$  as discussed. The quantum friction can be calculated by

$$F_x = -4\hbar \int_0^\infty \frac{d\omega}{2\pi} \int_{\omega/v}^\infty \frac{dk_x}{2\pi} \int_{-\infty}^\infty \frac{dk_y}{2\pi} \frac{k_x}{|\Delta|^2} ((k_\rho^2 - \beta k_0 k_x)^2 + \beta^2 k_z^2 k_y^2) e^{-2\text{Im}(k_z)d} ((k_\rho^2 - \beta k_0 k_x)^2 \times \text{Im}(r_{1p}) \text{Im}(r_{2p}') |D_{ss}|^2 - \beta^2 k_z^2 k_y^2 \text{Im}(r_{1p}) \text{Im}(r_{2s}') |D_{sp}|^2 + (p \leftrightarrow s)) \quad (\text{S43})$$

We recover the results in Ref. [11] which has a detailed calculation based on the stress tensor.

In the main text, we use the general theory here to generate the figures. At a fixed velocity  $10^4\text{m/s}$ , the critical distance is found to be  $10.04\text{nm}$  by Eq. (S41). In Fig. 3 of the main text,  $k_y$  in Eq. (S39) is integrated from  $-\infty$  to  $\infty$ . Here we show the 3D plots of Fig. 3 to illustrate the peak due to singular resonance more clearly.

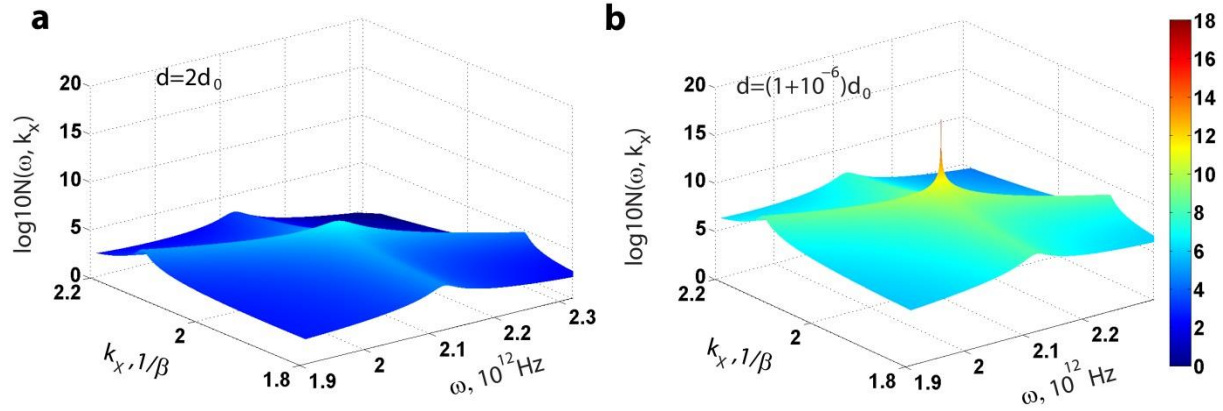


Figure S1. (a) and (b) are the three dimensional version of Fig. 3a and Fig. 3b in the main text, respectively. The large peak in (b) due to the singular resonance is evident. Even though the resonance condition occurs at a single isolated point in reciprocal space, it leads to divergences in physical observables.

In Fig. 4 of the main text, we have not integrated all the possible  $(\omega, k_x, k_y)$  region in Eq. (S43), but a neighborhood around the singularity  $(\omega_{SWR}, k_x^{PB}, k_y = 0)$ ,  $\omega$  from  $(1-0.05)\omega_{SWR}$  to  $(1+0.05)\omega_{SWR}$ ,  $k_x$  from  $(1-0.05)k_x^{PB}$  to  $(1+0.05)k_x^{PB}$ , and  $k_y$  from  $-0.05k_x^{PB}$  to  $+0.05k_x^{PB}$ . In Fig.4B, the magnitudes of quantum friction at  $d_1 = 2d_0$  and  $d_2 = (1+10^{-6})d_0$  are  $1.19 \times 10^{-6}\text{N/m}^2$  and  $0.280\text{N/m}^2$ , respectively.

## Divergence and the scaling law of quantum friction

We have shown that at the phase balance wavevector, the denominator  $\Delta_N$  of the integral Eq. (S43) can be exactly zero. Thus we have a three dimensional improper integral. We emphasize that this resonance condition leads to a divergence in quantum friction. Here, we rigorously prove the existence of this divergence and find the scaling law governing the quantum friction near the resonance condition. The analytical scaling law is in excellent agreement with the numerical calculations.

At a given velocity  $V$ , we first fix  $k_x$  to be the phase balance wavevector so that  $\Delta$  is real. At any distance  $d$ , we can find the minimum of  $\Delta_N$  as a function of  $\omega$  and  $k_y$  at  $(\omega^0, k_y^0)$ . We define  $d_0$  as the critical distance so that the minimum at  $d_0$  is zero. The minimum generally occurs at  $k_y = 0$  and  $\omega_{SWR}$ , but our derivation below does not depend on this statement of the location of the minimum. At the critical distance  $d_0$ , we have a singular point  $(\omega^0, k_x^{PB}, k_y^0)$  in three dimensional spaces  $(\omega, k_x, k_y)$  where the denominator  $\Delta_N$  is exact zero.

First we analyze the behavior of the denominator at this singular point. At the phase balance wavevector,  $\Delta_N$  is real valued as a function of  $\omega$  and  $k_y$ . As the function reaches the minimum, the first order derivatives of  $\omega$  and  $k_y$  are zero. However, the first order derivative of  $k_x$  is not zero but a complex number since  $\Delta$  is generally complex when  $k_x$  departs from  $k_x^{PB}$ . Therefore  $\Delta_N$  can be approximated by  $a_1\omega^2 + a_2k_y^2 + a_3k_x$  around the minimum. Here  $\omega$  should be understood by  $\omega - \omega_0$ , the difference to the singularity, so are  $k_y$  and  $k_x$ .  $a_1$  and  $a_2$  are positive numbers,  $a_3 = a_4 + ia_5$  is a complex number, the possible cross term  $\omega k_y$  is not important here since we are looking for an upper bound of  $\Delta_N$ . The denominator  $|\Delta_N|^2$  will be approximated by  $(a_1\omega^2 + a_2k_y^2 + a_4k_x)^2 + (a_5k_x)^2$ . In a neighborhood of the minimum, we have

$$1/2((a_1\omega^2 + a_2k_y^2 + a_4k_x)^2 + (a_5k_x)^2) < |\Delta_N|^2 < 2((a_1\omega^2 + a_2k_y^2 + a_4k_x)^2 + (a_5k_x)^2) \quad (\text{S44})$$

The sign of  $a_4$  here should be dealt with carefully. Firstly we consider the branch of  $k_x$  where  $a_4 k_x$  is positive. If  $a_4 > 0$ , we choose the branch  $k_x > 0$ ; if  $a_4 < 0$  we choose the branch  $k_x < 0$ . Then we have

$$\left(a_1 \omega^2 + a_2 k_y^2\right)^2 + (a_4 k_x)^2 \leq (a_1 \omega^2 + a_2 k_y^2 + a_4 k_x)^2 \leq 2\left(\left(a_1 \omega^2 + a_2 k_y^2\right)^2 + (a_4 k_x)^2\right) \quad (\text{S45})$$

For the asymptotic behavior, the constants  $a_i$  are not important. It is clear that there exists positive constants  $q$  and  $p$  so that,

$$q\left[(\omega^2 + k_y^2)^2 + k_x^2\right] < |\Delta_N|^2 < p\left[(\omega^2 + k_y^2)^2 + k_x^2\right]. \quad (\text{S46})$$

In the integral

$$\int d\omega dk_x dk_y \frac{1}{(\omega^2 + k_y^2)^2 + k_x^2}, \quad (\text{S47})$$

we first take  $\omega = r \cos \theta, k_y = r \sin \theta$ , so that the integral transforms to

$$\int dr^2 dk_x \frac{1}{(r^2)^2 + k_x^2} = \int dr dk_x \frac{1}{r^2 + k_x^2}. \quad (\text{S48})$$

Further by taking  $r = \rho \cos \theta, k_x = \rho \sin \theta$ , the integral will be

$$\int d\rho \frac{1}{\rho} \quad (\text{S49})$$

which diverges. Note that in the branch  $a_4 k_x < 0$ , the upper bound of  $|\Delta_N|^2$  in Eq. (S46) still satisfies; therefore the integral diverges in this branch also.

The scaling law can be seen just by an additional  $d - d_0$  term  $a_6 d$  ( $a_6$  is positive) in the first order Taylor expansion of  $\Delta_N$ . In a neighborhood of the minimum,

$$|\Delta_N|^2 \sim (a_1 \omega^2 + a_2 k_y^2 + a_4 k_x + a_6 d)^2 + (a_5 k_x)^2. \quad (\text{S50})$$

Following the same integration procedure, the integral will be

$$\int_0^\delta d\rho \frac{1}{\rho + d^2}, \quad (\text{S51})$$

where  $\delta$  is a constant that Eq. (S50) holds in the  $\delta$ -neighborhood. This integral gives

$$\ln \frac{1}{d} + \text{constant} . \quad (\text{S52})$$

Thus the scaling law will be

$$F(d) \propto \ln\left(\frac{d_0}{d-d_0}\right), \quad (\text{S53})$$

where we have replaced  $d$  by  $d-d_0$  and normalize it to  $d_0$ . It diverges very slowly as  $d$  approaches  $d_0$ .

### **Remarks on the limitations of the theory**

Till this point, we have shown the singular resonance leads to divergent dispersive force between the two plates in spite of loss of the material, polarization mixing as well as relativistic effects. However, non-local effects occur due to the large wavevector  $k_x$  and the close spacing between the plates [12]. Moreover, as the energy exchange between the two plates goes up, the large field intensity will cause nonlinear effects. In the theory part, we have essentially assumed the validity of linear scattering process. The fluctuational electrodynamics theory in Ref. [11] is based on linear response theory [13]. The nonlinear response of the media will certainly play an important role near the singular resonance. Thus we argue that non-locality and nonlinear effects will inevitably curtail the singularity.

### **The quantum friction varying with velocity**

The phase balance condition for the resonance is achieved by the coupling of positive and negative frequencies whereas the amplitude balance condition is adjusted by tuning the distance between the mirrors while keeping the velocity of the moving mirror fixed. In this section we show that changing the velocity while keeping the distance constant also leads to the excitation of the resonance. We also derive the scaling law with respect to the velocity at a given distance using a similar approach.

To prove the divergence of quantum friction and scaling law, we first fix the wavevector  $k_x$  to be the phase balance wavevector  $k_x^{PB}$ . The only difference is that  $k_x^{PB}$  is a function of the velocity, so

that it is also a variable compared to the given velocity case where  $k_x^{PB}$  (normalized to free space wavevector) is a constant. However, this fact will not affect the second step, finding the velocity where the minimum of the multi-reflection factor  $\Delta_N$  is exactly zero.

At all practical velocities,  $\Delta_N$  at the phase balance wavevector is well approximated by  $D_{pp}(k_x^{PB}) = 1 - |r_p(\omega)|^2 e^{-4\omega d/V}$  with  $k_x^{PB} = 2\omega/V$ . The minimum of  $D_{pp}(k_x^{PB})$  occurs at  $k_y = 0$  and  $\omega_{SWR}$  where  $|r_p(\omega)|$  has a resonance. That the minimum of  $D_{pp}(k_x^{PB})$  equals zero gives the critical velocity  $V_0$ ,

$$V_0 = d \frac{2\omega_{SWR}}{\ln|r_p(\omega_{SWR})|}. \quad (\text{S54})$$

Note that this equation is essentially the same to Eq. (S41). These two equations suggest that  $d/V$  should be a constant at the singular resonance. Certainly, the velocity given by Eq. (S54) should be practical.

The scaling law of quantum friction to the velocity approaching the critical velocity will be

$$F(V) \propto \ln\left(\frac{V_0}{V_0 - V}\right). \quad (\text{S55})$$

which can be easily read from the derivation of Eq. (S53). One can just replace  $d$  ( $d - d_0$ ) in Eq. (S50) by  $V$  ( $V_0 - V$ ).

Here we present the results when the vacuum gap is fixed at 10nm, and compare the photon exchange and quantum friction at different velocities. At this distance, the critical velocity  $V_0$  where the multi-reflection factor  $\Delta_N$  reaches zero is found to be  $0.996 \times 10^4$  m/s. Due to the same mathematical structure and similar parameters, the results here look close to that of fixed velocity case in the main text.

In Fig. S2, we plot the spectrum of photons exchanged according to their frequency and wavevector in the lab frame. For a distance  $V_1$  which is away from the singular Fabry-Perot Resonance condition of evanescent waves, we see two distinct bright regions in  $\omega - k$  space through which photons are spontaneously exchanged between the two plates. The vertical region corresponds to the surface wave resonance (SWR) frequency of the stationary plate where all

wavevectors are excited like in a conventional surface wave resonance. The curved region corresponds to the surface wave resonance frequency of the moving plate however the frequency is Doppler shifted and the region is curved instead of a straight line.

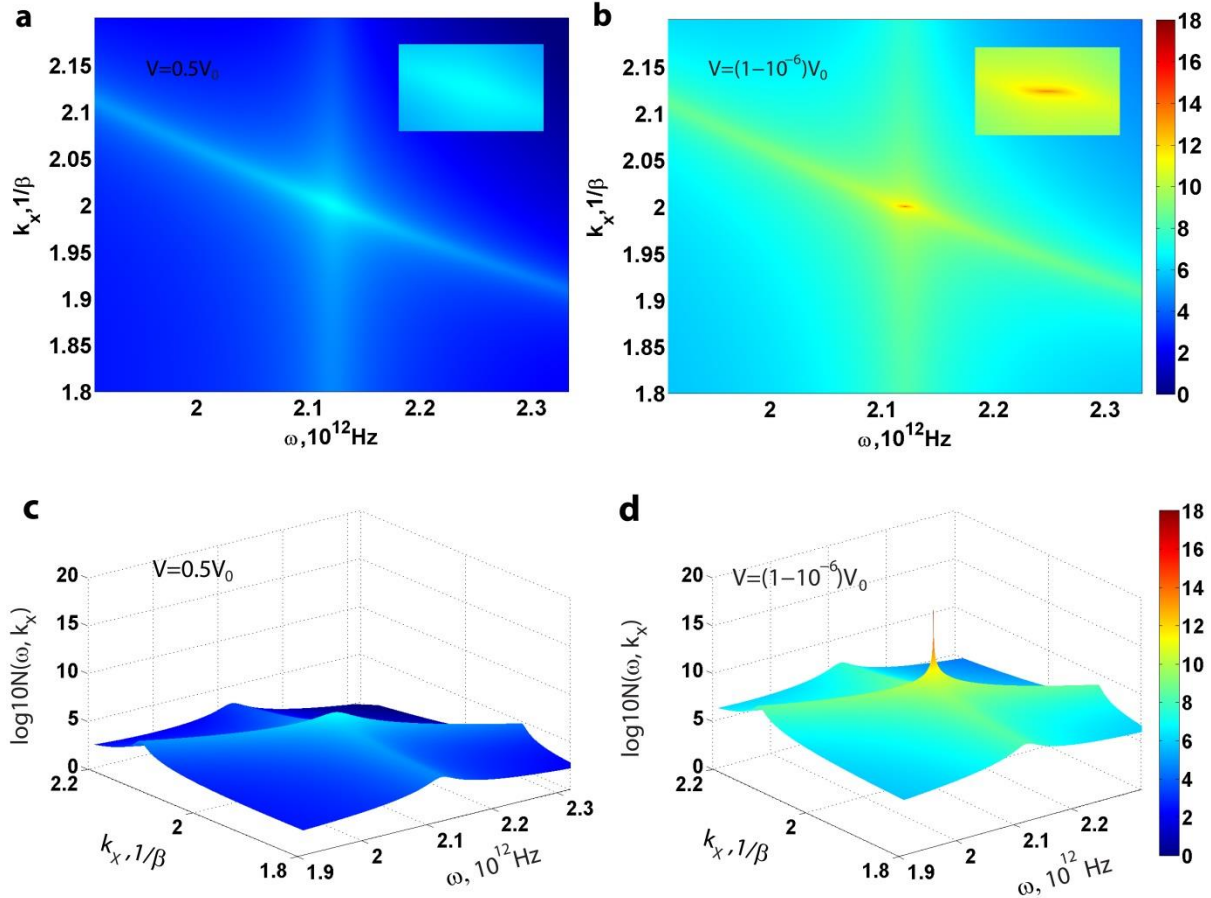


Figure S2. Contribution to exchanged photon number (in log scale) resolved by frequency and lateral wavevector  $k_x$  (normalized to free space wavevector) at (a)  $V=0.5V_0$  and (b)  $V \rightarrow V_0$ . In both (a) and (b), we see two bright curves, both of which are due to surface wave resonances. The vertical one comes from SWR at the interface of the stationary plate and vacuum while the other one is due to SWR at the interface of the moving plate and vacuum. These two bright curves join at the phase balance wavevector when the Doppler shifted SWR frequency in the co-moving frame is opposite to the SWR frequency in the lab frame. In (a), at a velocity much smaller than  $V_0$ , the singular resonance condition is far from being satisfied. However, the bright curves remain due to the SWR at the two interfaces. In (b), the red bright point is due to the singular resonance that arises since the amplitude balance condition is satisfied when  $V \rightarrow V_0$  and  $k_x = 2/\beta$ . This leads to giant photon exchange between moving plates at the phase and amplitude balance condition. The insets give the zoom in plots near the intersection of the two SWRs. We emphasize the dramatic increase in the photon exchange due to the singular FP resonance of evanescent waves. (c) and (d) are the three dimensional version of (a) and (b), respectively. The large peak in (d) due to the singular resonance is evident.

In Fig. S3(a), we plot the spectrum of the quantum friction force resolved according to the wavevector for various distances of the plates. The largest contribution to the force is due to the Fabry-Perot resonance of evanescent waves. When the velocity  $V$  approaches the critical distance  $V_0$ , the quantum friction  $F$  scales as  $\ln[V_0/(V_0 - V)]$ . We plot the friction vs. velocity in Fig. S3(b) to verify the theoretical predictions. The x axis is  $(1 - V/V_0)$  and in log scale. We clearly see the friction increases linearly as a function of  $\ln[V_0/(V_0 - V)]$  when  $V$  approaches  $V_0$ , consistent with the theoretical scaling law which predicts a divergence. In Fig. S3(b), the magnitudes of quantum friction at  $V_1 = 2V_0$  and  $V_2 = (1 - 10^{-6})V_0$  are  $9.65 \times 10^{-6} \text{N/m}^2$  and  $0.283 \text{N/m}^2$ , respectively.

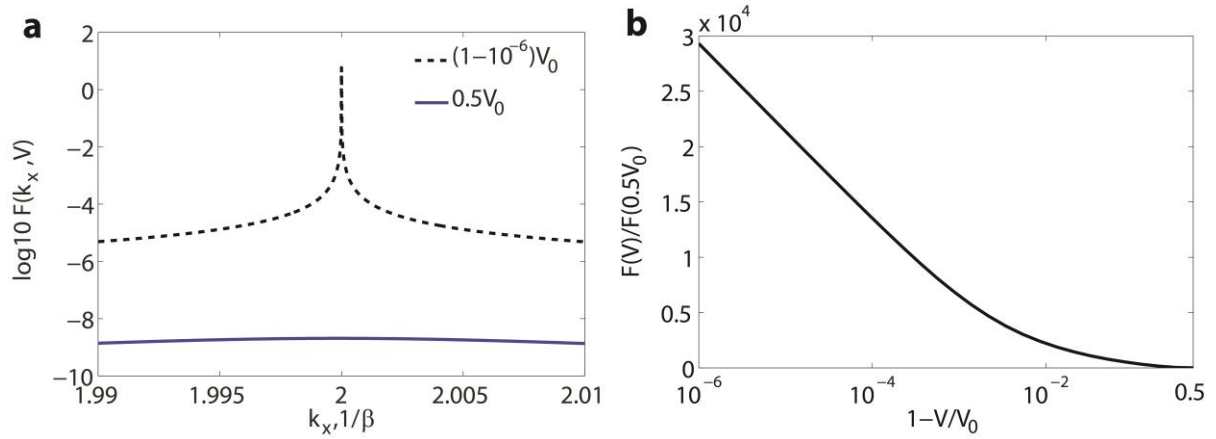


Figure S3. Quantum frictional force on the FP plates (a) resolved by the wavevector  $k_x$  at  $V = V_0^-$  and  $V = 0.5V_0$ . A major contribution to the force arises from modes at the perfect phase balance wavevector. However, at  $0.5V_0$ , the amplitude of friction is significantly smaller. (b) The distance dependence of friction at distances near  $V_0$ . The x axis is in  $(1 - V/V_0)$  and log scale. We clearly see a linear increasing behavior as  $V$  approaches  $V_0$ . This is consistent with the theoretical scaling law which predicts a logarithmic divergence of the quantum electrodynamic frictional force in the ideal limit.

## References

1. J. A. Kong, *Electromagnetic Wave Theory* (Wiley New York, 1990), Vol. 2.
2. J. B. Pendry, "Radiative exchange of heat between nanostructures," *J. Phys. Condens. Matter* **11**, 6621 (1999).
3. S.-A. Biehs, E. Rousseau, and J.-J. Greffet, "Mesoscopic Description of Radiative Heat Transfer at the Nanoscale," *Phys. Rev. Lett.* **105**, 234301 (2010).
4. M. F. Maghrebi, R. Golestanian, and M. Kardar, "Scattering approach to the dynamical Casimir effect," *Phys. Rev.* **87**, 025016 (2013).
5. L. Landau, E. Lifshitz, and L. Pitaevskii, *Electrodynamics of Continuous Media* (Pergamon Press, Oxford, 1984).
6. T. G. Philbin and U. Leonhardt, "No quantum friction between uniformly moving plates," *New J. Phys.* **11**, 033035 (2009).
7. M. F. Maghrebi, R. L. Jaffe, and M. Kardar, "Spontaneous Emission by Rotating Objects: A Scattering Approach," *Phys. Rev. Lett.* **108**, 230403 (2012).
8. M. Krüger, G. Bimonte, T. Emig, and M. Kardar, "Trace formulas for nonequilibrium Casimir interactions, heat radiation, and heat transfer for arbitrary objects," *Phys. Rev. B* **86**, 115423 (2012).
9. G. Bimonte, "Scattering approach to Casimir forces and radiative heat transfer for nanostructured surfaces out of thermal equilibrium," *Phys. Rev.* **80**, 042102 (2009).
10. L. Landau, E. Lifshitz, and L. Pitaevskii, *Statistical Physics, Part. 1* (Pergamon Press, Oxford, 1980), Vol. 24.
11. A. I. Volokitin and B. N. J. Persson, "Theory of the interaction forces and the radiative heat transfer between moving bodies," *Phys. Rev. B* **78**, 155437 (2008).
12. C. Cirac, R. T. Hill, J. J. Mock, Y. Urzhumov, A. I. Fernández-Domínguez, S. A. Maier, J. B. Pendry, A. Chilkoti, and D. R. Smith, "Probing the Ultimate Limits of Plasmonic Enhancement," *Science* **337**, 1072–1074 (2012).
13. R. Kubo, "Statistical-Mechanical Theory of Irreversible Processes. I. General Theory and Simple Applications to Magnetic and Conduction Problems," *J. Phys. Soc. Jpn.* **12**, 570–586 (1957).